Effect of the wave breaking mechanism on the momentum transfer

Alessandro Iafrati, INSEAN (Italian Ship Model Basin),
E-mail: a.iafrati@insean.it

1. INTRODUCTION

The flow generated by the breaking of free surface waves is numerically studied through a two-fluids Navier-Stokes solver. The aim is to investigate the differences in the vertical transfer of horizontal momentum induced by different breaking mechanisms.

The study has been stimulated by the concluding remarks in reported in Melville et al. (2002). Following an earlier work (Rapp and Melville, 1990), they used the dispersive focusing technique to produce plunging breaking waves and measured the velocity field. Through ensemble average, they distinguished the mean and the turbulent components and investigated the kinetic energy decay and the momentum flux. Consistently with the previous measurements of Rapp and Melville (1990), the kinetic energy, vorticity and the Reynolds stresses were found to decay like t^{-1}. However, estimates of the vertical transfer of horizontal momentum, were an order of magnitude less than those implied in the quasi-steady breaking past a hydrofoil (Duncan, 1981; Duncan and Dimas, 1996) and an order of magnitude larger than those estimated by Phillips et al. (2001) in the field of wind-generated waves.

The recent development of numerical approaches able to deal with complex free surface flows and topology changes of the interface, has widen the use of computational tools for such applications, see Scardovelli and Zaleski (1999) for a survey on the subject. What makes these tools very attractive is the possibility of achieving a very refined investigation of the flow field in a non-intrusive manner. This is particularly true in wave breaking flows with air entrainment as experimental measurements inside the bubbly flow is still a very challenging issue.

Despite the big development of the computational tools, important limits still remain as they are usually confined to low Reynolds numbers and two-dimensional flows. Nevertheless, results published so far have shown that a reasonably good agreement with the experimental observation can be achieved in terms of more global quantities. As an example, the breaking of steep free surface waves has been investigated in Chen et al. (1999). There it is shown that, soon after the plunging event, the energy takes a t^{-1} decay trend, which is in good agreement with the experimental findings by Melville et al. (2002). Moreover, it was found that about 80% of the initial wave energy is dissipated within three periods after the breaking. In a different context, Iafrati and Campana (2005) simulated the quasi steady breaking past a hydrofoil. Numerical simulations at different length scales have been performed, giving rise to different breaking regimes, ranging from plunging breaking up to microscale breaking waves in which the strong surface tension effects prevent the entrainment of air. In the latter case, it was found that a shear layer develops at the toe of the breaker and gives rise to coherent vorticity structures propagating downstream. An accurate analysis of the downstream propagating fluctuations has been done. The spectra of the fluctuations have been found in rather good qualitative and quantitative agreement with the experimental data by Walker et al (1996) and Duncan and Dimas (1996), although important differences in terms of decay properties of the fluctuations, presumably due to the two-dimensional assumption and to the much lower Reynolds number, have been noticed.

In the present paper a careful investigation of the wave breaking flow is carried out. The breaking of a rather steep wave in a periodic domain and the quasi-steady wave breaking flow past a submerged hydrofoil are carefully analyzed. The analysis is mainly focused at evaluating how deep the effects of the breaking, either in terms of air entrainment and horizontal momentum, do propagate into the water and how this changes with the breaking wave mechanism.

2. NUMERICAL MODEL

The study is carried out by using a two-fluids Navier-Stokes solver. It considers a single incompressible fluid with variable density and viscosity, so that the governing equations are

$$\begin{aligned} \nabla\cdot\boldsymbol{u} &= 0 \\ \frac{D\boldsymbol{u}}{Dt} &= -\frac{1}{\rho}\nabla p + \boldsymbol{f} + \frac{1}{\rho}\nabla\cdot\left[\mu(\nabla\boldsymbol{u}+\nabla\boldsymbol{u}^T)\right] \\ &\quad +\sigma\kappa\boldsymbol{\nu}\delta(\boldsymbol{x}-\boldsymbol{x}_s)\ , \end{aligned} \tag{1}$$

where ρ and μ are the local values of density and dynamic viscosity, respectively. In equation (1) p is the pressure, $\boldsymbol{f}$ denotes the mass forces, σ is the surface tension coefficient, κ is the local curvature of the interface and $\boldsymbol{\nu}$ is the unit normal vector at the interface oriented toward the air. In equation (1) the term $\delta(\boldsymbol{x}-\boldsymbol{x}_s)$ represents the Dirac function which is zero out of the interface location $\boldsymbol{x}_s$.

The system of Navier-Stokes equation is written in generalized variables and discretized onto a non stag-

gered grid. The system is solved through a fractional step approach: the momentum equation is advanced in time by neglecting pressure terms (*Predictor step*) whose effects are successively reintroduced by enforcing the continuity of the velocity field (*Corrector step*). The diagonal part of the dominating diffusive terms are accounted implicitly with a Crank-Nicolson scheme, whereas all the other viscous terms, related to the non uniformity of the viscosity and to the grid distortion, are computed explicitly. A low-storage, three-steps Runge-Kutta is adopted for the explicit terms. The Poisson equation for the pressure corrector term is solved with a multigrid accelerator coupled with a line Gauss-Seidel iterative procedure.

The interface is captured through a Level-Set algorithm. The signed distance d from the interface is reinitialized at each step and is convected with the transport equation:

$$\frac{\partial d}{\partial t} = -\boldsymbol{u} \cdot \nabla \boldsymbol{u} \ ,$$

which ensure that all particles belonging to the free surface ($d = 0$) continue to stay there, as the kinematic boundary condition requires. The surface tension contribution to the momentum equation is approximated by a continuum model as suggested in Brackbill et al. (1992).

The numerical model has been deeply validated and verified in Iafrati and Campana (2005) where a more detailed description of the numerical model is also presented.

3. BREAKING OF A STEEP WAVE IN A PERIODIC DOMAIN

As a first example, a rather steep gravity water wave, is initialized in a computational domain with periodic boundary conditions. The extension of the computational domain is one wavelength in both horizontal and vertical directions. As a validation step, a calculation is done in the same conditions used in Chen et al. (1999). The air/water density ratio is 0.01 and the ratio of dynamic viscosities of air and water is 0.4.

The free surface shape is initialized as

$$\eta(x,0) = a\cos(kx) + \frac{1}{2}a^2 k\cos(2kx) + \frac{3}{8}a^3k^2\cos(3kx) \ ,$$

where $k = 2\pi$, being $\lambda = 1$ the horizontal extension of the computational domain. The steepness ak is fixed to a very high value $ak = 0.55$. At $t = 0$ the velocity field in water is initialized on the basis of the velocity potential

$$\phi(x,y,t) = \frac{ga}{\omega}e^{ky}\sin(kx - \omega t) \ ,$$

where $\omega = \sqrt{gk(1 + k^2a^2)}$ is used to account for second order dependence on the wave steepness.

The time sequence of the free surface profiles reported in Fig. 1 shows the progressive steepening of the wave, the development and the plunging of the jet, the splash up formation and the entrainment of air bubbles. As time elapses, the energy is gradually dissipated and the free surface disturbances are progressively smoothed out.

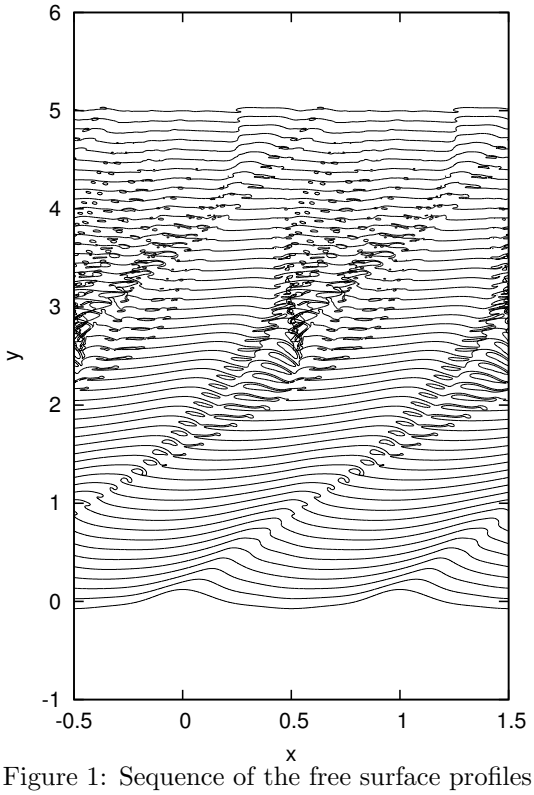

Figure 1: Sequence of the free surface profiles of a steep gravity wave in a periodic domain $x \in [-0.5, 0.5]$. A vertical shift equal to the corresponding time instant is applied at each profile. The periodic profile on the right hand side ($x \in [0.5, 1.5]$) is also drawn to make it clearer the dynamics of the breaking process and of the bubble entrainment.

With the aim of showing how deep propagate into the water the effects of the breaking process on the velocity field, in Fig. 2 three successive configurations are displayed. In those pictures, color coded vorticity contours and the free surface shape are drawn. For the sake of clarity, the vorticity distribution is shown in water only. This sequence shows how the large bubble entrained in progressively squeezed and then fragmented into smaller bubbles which are successively pushed up toward the free surface both by the combined action of the velocity field and of the buoyancy. It is worth noticing that, although the strong rotational flow is primarily induced by the plunging process, in the late stage relevant vorticity structures (rotating clockwise) develops beneath the free surface. It is believed that this

structures are generated by the current, moving toward the right, developing in the upper water layer.

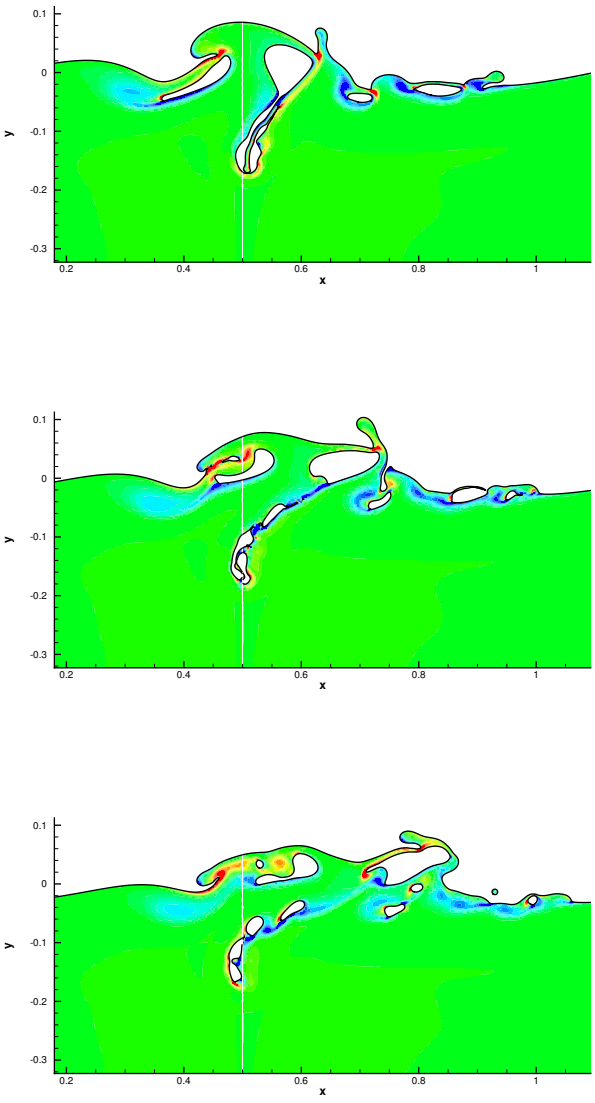

Figure 2: The late stage of the breaking when the big air bubble is split into smaller ones. Colored contours represents the vorticity field, which are drawn in water only. The thin white line about $x = 0.5$ is the boundary of the (periodic) computational domain.

In order to estimate the accuracy of the results, two different calculations have been carried out, on 256×256 and 512×512 grids. In the early stage the two solutions are about overlapped but, as soon as the jet develops, the finer grid provide a faster jet and then a different dynamics of the breaking process. This disagreement, which is not shown here, has been also observed in Chen et al. (1999).

In spite of the remarkable difference in the dynamics of the breaking process, the overall behaviour of the energy is in a rather good agreement (Fig. 3). It can be seen that a t^{-1} is approached in both cases soon after the breaking event. It is worth remarking that the above results are rather preliminary and a deeper investigation on the role played by numerical parameters, such as the thickness of the transition region used to smooth the jump in the fluid properties, is needed.

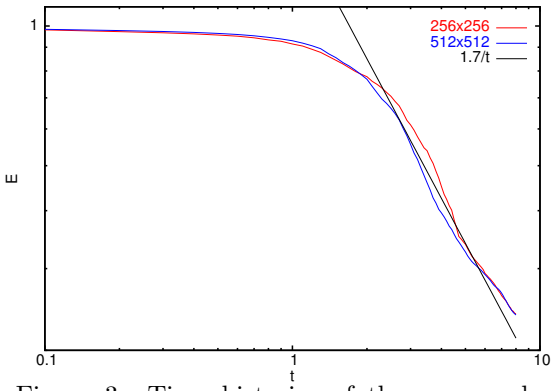

Figure 3: Time histories of the energy obtained by numerical simulations on a 256 × 256 and on a 512 × 512 grid. The t^{-1} power law is also drawn.

4. QUASI-STEADY BREAKING WAVE PAST A SUBMERGED HYDROFOIL

With the aim of addressing the question raised in Melville et al. (2002), in addition to the breaking of the steep gravity wave, the quasi-steady spilling breaking flow past a submerged hydrofoil is investigated further. This problem has been widely studied in Iafrati and Campana (2005), with attention mainly focused at the differences in the breaking wave establishment mechanisms and in the free surface fluctuations. Here the unsteady velocity field is analyzed more carefully.

In fact, the quasi-steady flow is characterized by a shear layer developing at the toe of the breaker instability of which gives rise to coherent cortical structures propagating beneath the free surface. The continuous interaction between the coherent structures and the air-water interface is responsible for the downstream propagating fluctuations. On the basis of the considerations in Melville et al. (2002) and in Phillips et al. (2001) concerning the estimate of the momentum flux, the velocity fields at different times are post-processed and the mean and fluctuating components are derived. In Fig. 4 the contour of the $\overline{u'v'}$ are drawn. As it happens for the shear layers, $\overline{u'v'}$ takes large (and positive) values in a long region attached to the toe. Further downstream this quantity progressively vanishes and takes

again positive values beneath the first trough.

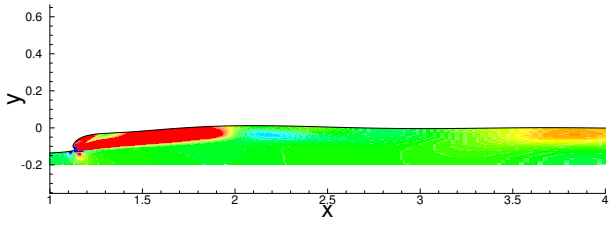

Figure 3: Plot of the averaged free surface position along with the contour of the $\overline{u'v'}$ with the thick red zone indicating the region with the rapid growth of the coherent structures.

5. CONCLUDING REMARKS

Numerical results about wave breaking flows generated in different ways have been shown and briefly discussed. The final objective of the work is to investigate the vertical transfer of the horizontal momentum and the differences in the momentum fluxes associated to the different breaking types. At this stage only a rather preliminary study has been presented while a more careful analysis should be presented at the Workshop.

6. ACKNOWLEDGEMENTS

The present activity has been done within the framework of the "Programma di Ricerca Idrodinamica Navale 2005-07" funded by *Ministero delle Infrastrutture e dei Trasporti*.

7. REFERENCES

J.U. Brackbill, D.B. Kothe and C. Zemach (1992) *A continuum method for modeling surface tension*, J. Comput. Phys., **100**, 335.

G. Chen, C. Kharif, S. Zaleski and J. Li (1999) *Two-dimensional Navier–Stokes simulation of breaking waves*, Phys. Fluids, **11**, 121.

J.U. Duncan (1981) *An experimental investigation of breaking waves produced by a towed hydrofoil*, Proc. Roy. Soc. London, **A377**, 331.

J.U. Duncan and A.A. Dimas (1996) *Surface ripples due to steady breaking waves*, J. Fluid Mech., **329**, 309.

A. Iafrati, E.F. Campana (2005) *Free surface fluctuations behind microbreakers: space–time behaviour and subsurface flow field*, J. Fluid Mech., **529**, 311.

W.K. Melville, F. Veron and C.J. White (2002) *The velocity field under breaking waves: coherent structures and turbulence*, J. Fluid Mech., **454**, 203.

O.M. Phillips, F.L. Posner and J.P. Hansen (2001) *High range resolution radar measurements of the speed distribution of breaking events in wind-generated ocean waves: surface impulse and wave energy dissipation rates*, J. Phys. Oceanogr., **31**, 450.

R.J. Rapp and W.K. Melville (1990) *Laboratory measurements of deep-water breaking waves*, Phil. Trans. R. Soc. London, **A331**, 735.

R. Scardovelli, S. Zaleski, S. (1999) *Direct numerical simulation of free surface and interfacial flow*, Annu. Rev. Fluid Mech., **31**, 567.

D.T. Walker, D.R. Lyzenga, E.A. Ericson and D.E. Lund (1996) *Radar backscatter and surface roughness measurements for stationary breaking waves*, Proc. Roy. Soc. London, **A 452**, 1953.